ResearchGate

See discussions, stats, and author profiles for this publication at: https://www.researchgate.net/publication/269465854

Ribonuclease A adsorption onto charged self-assembled monolayers: A multiscale simulation study

ARTICLE *in* CHEMICAL ENGINEERING SCIENCE · JANUARY 2015

Impact Factor: 2.34 · DOI: 10.1016/j.ces.2014.07.021

CITATIONS
5

READS
41

3 AUTHORS, INCLUDING:

Jian Zhou
South China University of Technology
84 PUBLICATIONS **1,592** CITATIONS

SEE PROFILE

Available from: Jian Zhou
Retrieved on: 24 January 2016

Chemical Engineering Science 121 (2015) 331–339

Contents lists available at ScienceDirect

Chemical Engineering Science

journal homepage: www.elsevier.com/locate/ces

Ribonuclease A adsorption onto charged self-assembled monolayers: A multiscale simulation study

Jie Liu, Gaobo Yu, Jian Zhou*

School of Chemistry and Chemical Engineering, Guangdong Provincial Key Lab for Green Chemical Product Technology, South China University of Technology, Guangzhou 510640, PR China

HIGHLIGHTS

- Ribonuclease A adsorption orientation is studied by multiscale simulations.
- The catalytic activity can be enhanced when ribonuclease A is adsorbed on NH_2-SAM.
- The catalytic activity of ribonuclease A is screened when it is adsorbed on COOH-SAM.
- Negatively charged surfaces could be used for ribonuclease A removal.
- Positively charged surfaces can be used for the immobilization of ribonuclease A.

GRAPHICAL ABSTRACT

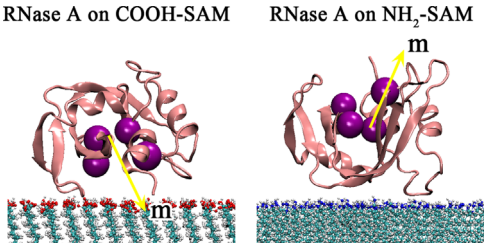

ARTICLE INFO

Article history:
Received 20 March 2014
Received in revised form
25 June 2014
Accepted 12 July 2014
Available online 17 July 2014

Keywords:
Protein adsorption
Protein orientation
Enzyme immobilization
Multiscale
Molecular dynamics simulation
Coarse-grained simulation

ABSTRACT

An ordered adsorption orientation is significant for the catalytic activity of immobilized enzymes. In this study, the orientations and conformation of ribonuclease A (RNase A) adsorbed on oppositely charged self-assembled monolayers (SAM) have been studied by a multiscale approach, including parallel tempering Monte Carlo, all-atom molecular dynamics and coarse-grained molecular dynamics simulations. Simulation results show that RNase A adsorbed on oppositely charged surfaces with opposite orientations. The active site of RNase A is oriented toward the surface when it adsorbs on a negatively charged surface; while for RNase A adsorbed on a positively charged surface, the active site is oriented toward the solution. Negatively charged surfaces could be used for RNase A removal since the catalytic active site is blocked. To bring the enzymatic catalysis of RNase A into play, positively charged surfaces can be used to control the orientation of RNase A with the active site accessible. The dipole moment and side chains of RNase A on both surfaces are slightly changed, whereas the backbone structure of RNase A is well preserved. That is to say, RNase A preserves its native conformation during the adsorption process. The simulation results could be applied into the design and development of substrates for the immobilization of ribonuclease A.

© 2014 Elsevier Ltd. All rights reserved.

1. Introduction

Enzyme adsorption on surfaces plays an important role in many biological processes (Secundo, 2013; Zhang et al., 2009; Khan and Garnier, 2013). The bioactivity of enzyme on surfaces mainly depends on the orientation and conformation of enzymes after adsorption. Ribonucleases (RNases) are a class of enzymes that can catalyze the cleavage of phosphodiester bonds in RNA (Glennon and Warshel, 1998). Thus, the immobilization of RNases on solid surfaces with ordered orientation is vital in many applications, such as purification of biopharmaceutical plasmid DNA (Cullen et al., 2008).

* Corresponding author. Tel./fax: +86 20 87114069.
E-mail address: jianzhou@scut.edu.cn (J. Zhou).

http://dx.doi.org/10.1016/j.ces.2014.07.021
0009-2509/© 2014 Elsevier Ltd. All rights reserved.

Ribonuclease A (RNase A) (Findlay et al., 1961; Cuchillo et al., 2011) is a monomeric enzyme that catalyzes the transphosphorylation of single-stranded RNA without using cofactors or metal ions (Ji and Zhang, 2011). RNase A is usually used for RNA degrading. However, RNase A was purified from bovine pancreas and regulatory authorities recommend that bovine derived materials should be avoided in the production of bio-therapeutics, following the outbreak of new-variant Creutzfeld–Jakob disease in the UK (Eon-Duval and Burke, 2004; Cooke et al., 2001). It is necessary to avoid the appearance of free RNase A in the solution. Thus, lots of researchers investigated chemically modified materials to remove (Yi et al., 2008), inactivate or immobilize (Cullen et al., 2008) RNase A. Among these studies, most researchers focused on the stability of RNase A adsorption on charged surfaces. Siegel and coworkers (Shang et al., 2007) reported the unfolding behavior of RNase A on silica nanoparticle surfaces and quantitatively demonstrated that nanoscale size and surface curvature played key roles in influencing the stability of adsorbed proteins. The thermodynamic stability of RNase A decreased after adsorption onto the nanoparticles, since nanoparticles increased the surface contact area and surface-protein interactions increased. Subsequently, they studied the influence of nanoparticle curvature and protein structure on the orientation of proteins which adsorbed on the silica nanoparticles (Shrivastava et al., 2012). Yi et al. (2008) figured that RNase A was less active on the carbon nanotube surface functionalized with carboxylic groups than in free solution; the activity was decreased further on larger carbon nanotubes. Cullen et al. (2008) employed poly(acrylic acid) (PAA) brushes as templates to immobilize RNase A. They detected that, as the thickness of the brush increased, the surface density of RNase A increased monotonically. Wittemann and Ballauff (2005) investigated the thermal unfolding and refolding behavior of RNase A adsorbed to spherical polyelectrolyte brushes with negative charges. Becker et al. (2011) found that, at low ionic strength, RNase A was strongly adsorbed by the spherical polyelectrolyte brush particles despite the fact that both particles and the protein are positively charged. Smith et al., (2005) produced a high-density poly-(vinylsulfonate) coating which sequestered RNases from aqueous solutions quickly and completely. Meanwhile, this coating could be used to maintain the integrity of ribonucleic acids in a variety of contexts.

As the orientation and binding sites of enzyme adsorption on the atomic level are difficult to be obtained from experiments, molecular simulation provides an alternative to study protein behaviors on surfaces Mijajlovic et al., 2013. Zhou et al. (2003, 2004a) developed a generalized residue-based model to predict the orientation of antibodies on charged surfaces. A combined Monte Carlo (MC) and molecular dynamic (MD) study was used to investigate the orientation and conformation of cytochrome c adsorbed on self-assembled monolayers (Zhou et al., 2004b). However, conventional MC and MD simulations in canonical ensemble often suffer from the quasi-ergodic problem, i.e., simulations at low temperatures tend to get trapped in local-minimum-energy states and thus fail to sample the whole configuration space (Xie et al., 2010). Xie et al. (2010) developed a parallel tempering Monte Carlo (PTMC) algorithm, which was based on the united-residue model (Zhou et al., 2003) in implicit solvent, to solve this problem. With the preferred orientation predicted by PTMC as initial configuration, further atomistic mechanisms including the interactions between proteins and surfaces, binding sites, conformation changes could be investigated by MD simulations.

All-atom molecular dynamics (AAMD) can provide more detailed information in the atomistic level, though it is still restricted within the microsecond time scale to investigate the protein adsorption process (Wei et al., 2011; Liang et al., 2012; Mijajlovic and Biggs 2007). Coarse-grained molecular dynamics (CGMD) simulations (Monticelli et al., 2008; Marrink et al., 2007; Marrink et al., 2003; Lopez et al., 2009, 2013) could sample the dynamics of soft matters on longer time scales and larger length scales. CGMD simulations are performed to investigate whether a reorientation is occurred at the microsecond timescale.

Previous works about RNase A were focused on the adsorption amount; however the orientation of RNase A on charged surfaces, which is very important for the bioactivity of enzymes, had not been paid sufficient attentions yet. The fundamental microscopic mechanism of RNase A adsorption on charged surfaces are not clear also. In order to study the influence of surface chemistry on the orientation and conformation changes of adsorbed proteins, self-assembled monolayers (SAMs) functionalized with different chemical groups, were usually used (Wei et al., 2011; Xie et al., 2012; Sheng et al., 2010; Yu et al., 2012; Trzaskowski et al., 2005; Xie et al., 2013; Agashe et al., 2005; Hsu et al., 2008; Wang et al., 2006; Nordgren et al., 2002; Trzaskowski et al., 2008; Liu et al., 2013; Ostuni et al., 1999).

In this work, we combine PTMC with AAMD and CGMD to investigate the orientations of RNase A adsorbed on oppositely charged SAMs and to obtain a more detailed atomistic understanding of RNase A adsorption on charged surfaces. The PTMC method is used to get the primary orientation of RNase A on different charged surfaces. Then, the AAMD is adopted to study the atomistic mechanism of the interactions between RNase A and charged surfaces. Finally, RNase A adsorption is further investigated by CGMD simulation in microsecond time scale to examine the protein orientation in a longer time scale. RNase A solvated in bulk is also studied as a reference system. The orientation and conformation changes during RNase A adsorption are examined. The rational control requirements, to enhance the bioactivity of RNase A or to remove it, are illustrated in detail .

2. Simulation details

RNase A has 124 residues. It consists of three alpha-helices and six beta-strands with a cleft (Ji and Zhang, 2011). The active site of RNase A is mainly constituted by His12, Lys41, His119, Asp121 residues (Camilloni et al., 2012). The high-resolution crystal structure of RNase A (Wlodawer et al., 1988) (PDB ID: 7RSA) obtained from the RCSB (www.pdb.org) is shown in Fig. 1.

2.1. PTMC

The main purpose of PTMC (Xie et al., 2010) was to get the preliminary preferred orientation of RNase A adsorbed on charged surfaces, which can be used as the initial orientation in MD studies. According to the united-residue model (Zhou et al., 2003), each amino acid within RNase A was reduced to a sphere centered at the α-carbon atom of the residue. The protein was kept rigid during PTMC simulations. The charged surface was treated as a flat surface. There are van der Waals (vdW, U_{vdw}) and electrostatic interactions (U_{ele}) between the charged surfaces with protein. The parameters were taken from our previous works (Zhou et al., 2003; Xie et al., 2010; Liu et al., 2013). RNase A was initially put in the center of the simulation box, then with translational and rotational moves around its center of mass. 40,000,000 MC cycles were carried out with 20,000,000 cycles for equilibration and another 20,000,000 cycles for production. Six replicas, with temperatures of 300 K, 350 K, 400 K, 480 K, 580 K and 700 K, respectively, were used to ensure sufficient energy overlap between neighboring replicas. The swaps are performed every 500 cycles. The final protein orientation with the lowest energy

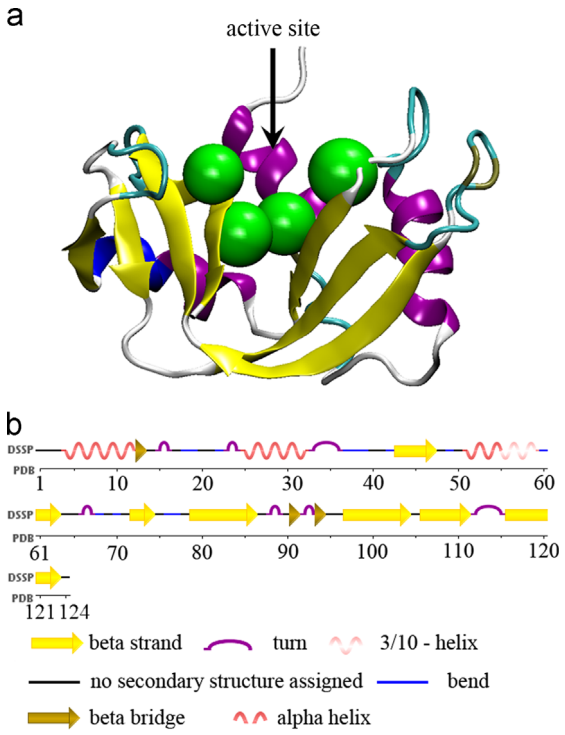

Fig. 1. (a) Secondary structure of RNase A. Green beads represent the active site in RNase A. Image (b) is from RCSB PDB (www.pdb.org) for RNase A (PDB ID: 7RSA). (For interpretation of the references to color in this figure legend, the reader is referred to the web version of this article.)

was taken as the initial configuration for further MD simulations (Liu et al., 2013).

2.2. CGMD

Recently, the CG model based on MARTINI force field was applied to study the interactions between proteins and biomaterials (Liang et al., 2012; Hung et al., 2011; Yu et al., 2014). In order to get more accurate electrostatic interactions between the protein and charged surfaces, the combination of MARTINI force field for protein (Monticelli et al., 2008; Marrink et al., 2007) and BMW water model (Wu et al., 2010, 2011) was used in this study.

In CGMD simulations, all systems were simulated by the combination of MARTINI (version 2.1) force field (Monticelli et al., 2008; Marrink et al., 2007) and BMW water model (Wu et al., 2010). The CG structure of RNase A was created by mapping most amino acids onto single standard particle types (Marrink et al., 2007). The backbone structure and secondary structures of RNase A were preserved after coarse-graining. As the CGMD we performed here was used to investigate the orientation of protein, the Elastic Network model (Periole et al., 2009) was adopted to avoid the unusually conformation change of coarse-grained proteins.

The charged surfaces were constructed to mimic charged SAMs. The outermost charged groups were represented by charged beads (Q_a for negatively charged terminus and Q_d for positively charged terminus) in CGMD; while the other groups were represented by C1 beads to mimic the alkyl chains of SAMs (Yu et al., 2014). The charged density of the surface was the same as that used in AAMD, which is 0.05 C/m^2. The surfaces were kept fixed during the whole simulations. The initial orientations of adsorbed RNase A were taken from PTMC results.

CGMD simulations in a canonical ensemble were performed to examine the adsorption behaviors of RNase A by using GROMACS 4.5.4 package (Hess et al., 2008). It is worth noting that, due to the smoothed energy barrier in the MARTINI force field, the effective time that the system goes through is four times longer than the simulation sampling time (Monticelli et al., 2008). 1.2 μs CGMD simulation was performed for each system. The simulation box size was $7.52 \times 7.52 \times 10.23$ nm^3. The periodic boundary conditions were applied only in x and y directions. The integrating time step was 20 fs. The temperature was controlled by a Nose–Hoover thermostat (Hoover 1985; Nose 1984) with a time constant of 4.0 ps. The temperature of the simulated system was 300 K. Electrostatic interactions were calculated by the Particle mesh Ewald method (Essmann et al., 1995) with a spacing of 0.2 nm and $\varepsilon_r = 1.3$. For vdW interactions, switching functions were used from 0.9 nm to 1.2 nm. For water–water vdW interactions, the switch scheme ($r_{shift} = 0.9$ nm and $r_{cut} = 1.4$ nm) is used.

2.3. AAMD

For MD simulations, the initial orientations of RNase A were also from PTMC simulations. Hydrogen atoms within the protein were added by GROMACS 4.5.4 (Hess et al., 2008). RNase A was simulated at pH 7.0. All acidic amino acids (i.e., glutamate and aspartate) and the C-terminus of RNase A were deprotonated, while basic amino acids (i.e., lysine and arginine) along with the N-terminus were protonated. For the protonation states of histidine residues, (Merlino et al., 2002) His12 and His48 were protonated at $N^{\delta 1}$, whereas His105 and His119 were protonated at $N^{\varepsilon 2}$. With these settings, the net charge of RNase A was +4 e. The potential parameters for proteins are from the OPLS force field (Kaminski et al., 2001).

The $HS(CH_2)_{10}COOH$ SAM and $HS(CH_2)_{10}NH_2$ SAM on Au(111) with $\sqrt{3} \times \sqrt{3}$ structures (Zhou et al., 2004b) were adopted in the all-atom MD simulations. There are totally 196 thiol chains and 1764 gold atoms; the sulfur atoms of the thiol chains and all gold atoms were kept fixed during AAMD simulations. For thiol chains in the studied systems, 14 chains were randomly selected for protonation or deprotonation, representing a surface charge density of 0.05 C/m^2 to mimic to the experiment. The surface had the dimension of 6.99×6.06 nm^2. The potential parameters for SAMs were from the OPLS force field (Kony et al., 2002).

Water molecules were added to the simulation box, with the dimension of $6.99 \times 6.06 \times 7.00$ nm^3, in which there was a single RNase A. The added water molecules were selected such that no water oxygen atom was closer than 0.28 nm to the protein. There were 9100–9300 water molecules within the simulation boxes for different systems. The water molecules were described by the SPC/E model (Chatterjee et al., 2008). Counter ions (Na^+ and Cl^-) were added to keep the system neutral. The simulation box size was $6.99 \times 6.06 \times 9.90$ nm^3, in which SAMs were 2.8 nm high. The periodic boundary conditions were only used in x and y directions (Yeh and Berkowitz, 1999). Before MD simulations, each system was optimized with the steepest descent method and conjugate gradient method to eliminate the steric overlap or inappropriate geometry after converting the coarse-grained structure into the atomistic structure (Trzaskowski et al., 2008), as the side chain of protein was ignored in PTMC simulations. With the GROMACS 4.5.4. package (Hess et al., 2008), NVT-MD simulations were performed. The integrating time step was 2 fs. The temperature was controlled by a Nose–Hoover thermostat (Hoover, 1985; Nose, 1984) with a time constant of 0.4 ps. The temperature of the simulated system was 300 K. The LINCS algorithm was performed to constrain the bonds containing hydrogen atoms (Hess et al., 1997). The cutoff distance was 1.0 nm for the non-bonded interactions. Electrostatic interactions were calculated by the Particle mesh Ewald method (Essmann et al., 1995) for a slab system. 50 ns MD simulation was performed for each system. RNase A solvated in bulk was performed also as a reference for

comparison. The periodic boundary conditions of RNase A in bulk were used in 3-dimensional directions. Other running parameters of bulk system were the same as mentioned for surface systems. For structure visualization, the visual molecular dynamics (VMD) program (Humphrey et al., 1996) was used. The electrostatic profile of RNase A was calculated by the Chimera package developed by UCSF (Pettersen et al., 2004).

3. Results and discussion

The orientation and conformation of RNase A adsorbed on charged SAM surfaces were studied by multiscale simulations (PTMC, AAMD and CGMD). The possible catalytic activity is analyzed by the obtained orientation and conformation changes of RNase A on charged surfaces. Simulation results are summarized in Tables 1–2 and Figs. 2–8.

3.1. Energy and orientation

The adsorption energies between RNase A and charged surfaces, obtained from AAMD, are shown in Table 1. It provides the driving force information which dominates the protein adsorption. As shown in Table 1, RNase A adsorbed on both kind of surfaces are driven by the competition between electrostatic and vdW interactions. The electrostatic interaction energy of RNase A adsorbed on COOH-SAM is distinctly higher than that on NH_2-SAM. It is mainly caused by the net charge of RNase A, +4 e. Thus, the dominant driving force of RNase A adsorbed on COOH-SAM is electrostatic interaction; while RNase A on NH_2-SAM is driven by both electrostatic and vdW interactions. On both charged surfaces, the vdW interactions still play a role and cannot be ignored. That means, on charged hydrophilic surfaces, the hydrophobic interactions also contribute to the protein adsorption.

The protein orientation is quantitatively characterized by the orientation angle, (Zhou et al., 2003, 2004a, 2004b; Xie et al., 2010; Liu et al., 2013) which is defined as the angle between the unit vector normal to the surface (**n**) and the unit vector along the protein dipole (**m**). The cosine value of this angle is used to quantitatively represent the orientation of the adsorbed protein.

Table 1
Interaction Energies of RNase A Adsorbed on Charged Surfaces by AAMD.

	U_{tot} (kJ mol^{-1})[a]	U_{vdw} (kJ mol^{-1})	U_{ele} (kJ mol^{-1})
RNase A on COOH-SAM	−685.8	−126.9	−558.9
RNase A on NH_2-SAM	−303.9	−106.7	−197.2

[a] U_{tot} represents the sum of electrostatic and vdW interactions.

Table 2
Averaged properties of the RNase A in bulk solution and adsorbed on SAM surfaces by MD simulations.

	Orientation[a]	R_{gyr} (nm)	Eccentricity	RMSD (nm)	Dipole (D)
Bulk	–	1.44 ± 0.01	0.14	0.31	311 ± 33
On COOH-SAM by AAMD	−0.80	1.47 ± 0.01	0.20	0.23	466 ± 21
On NH_2-SAM by AAMD	0.88	1.48 ± 0.01	0.18	0.24	472 ± 36
On COOH-SAM by CGMD	−0.82	1.45 ± 0.01	0.19	–	460 ± 30
On NH_2-SAM by CGMD	0.94	1.44 ± 0.01	0.17	–	494 ± 32

[a] Orientation refers to the cosine value of the angle between the dipole and the surface normal.

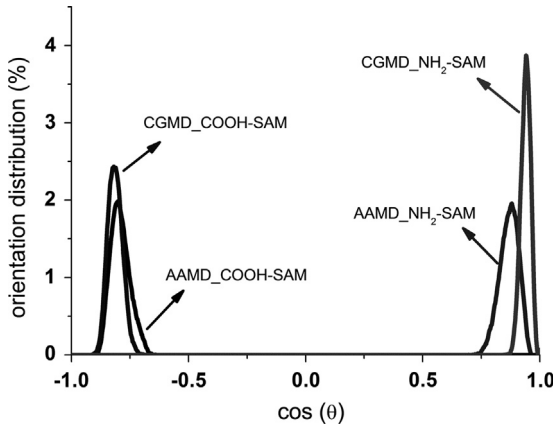

Fig. 2. Orientation distributions of RNase A adsorbed on COOH-SAM and NH_2-SAM simulated by AAMD and CGMD.

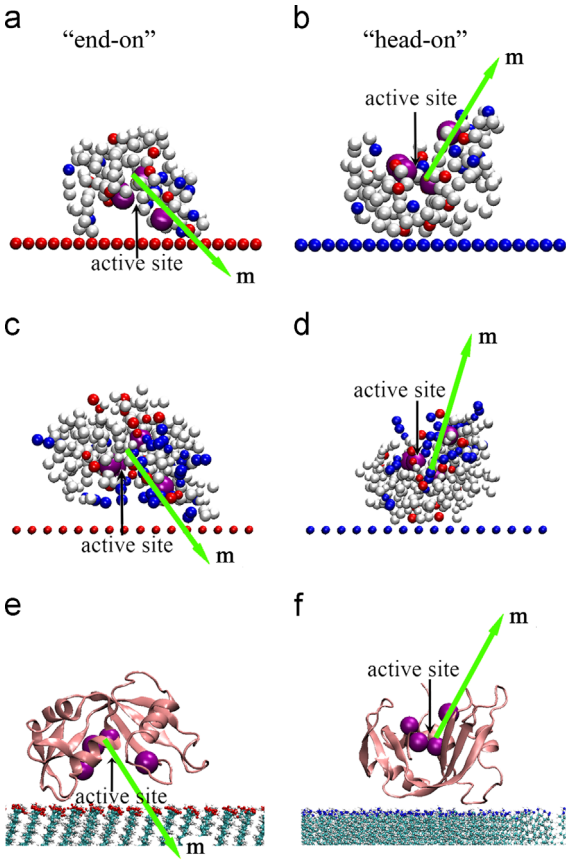

Fig. 3. Preferred configurations of protein orientations on COOH-SAM ((a), (c), (e)) and NH_2-SAM ((b), (d), (f)) from PTMC (above), CGMD (middle) and AAMD (below) simulations. The direction of dipole of RNase A is noted as **m**. Red beads represent negatively charged residues; blue beads represent positively charged residues; purple beads represent the active site in RNase A. The surface with top red groups is for COOH-SAM while that with blue top groups is for NH_2-SAM. (For interpretation of the references to color in this figure legend, the reader is referred to the web version of this article.)

Orientation distributions of RNase A on different charged surfaces during CGMD and AAMD simulations are shown in Fig. 2 and Table 2. In PTMC, the simulations were based on the united-residue model, in which the side chains of the protein were ignored. The dipole moment calculated in PTMC deviates a little bit from that in AAMD. The orientation obtained from PTMC was used as the preliminary preferred protein orientation in MD simulations. The orientation distributions in both CGMD and AAMD present the same trend (as shown in Fig. 2), which indicates

that, for both kinds of surfaces, RNase A gets the global-energy-minimum orientation state. The representative adsorption snapshots of RNase A on SAMs are shown in Fig. 3. RNase A could adsorb on different charged surfaces in opposite orientations. In another word, the orientation of RNase A can be controlled by regulating the charge property of the carrier for immobilization.

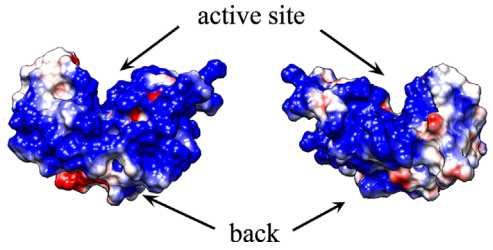

Fig. 4. The electrostatic maps of RNase A in front and back views.

For COOH-SAM surface, RNase A is adsorbed with "end-on" orientation (i.e., the active site orients toward the surface). As the active site of RNase A orients towards the surface, the catalytic capacity of RNase A is blocked. Lee et al. (Lee and Belfort, 1989) detected that, on the initial adsorption, the activity of enzyme molecules above the negatively charged mica surface were completely screened. Yi et al. (2008) found that multi-walled carbon nanotubes and single walled carbon nanotubes functionalized with carboxylic groups could interact with RNase A and cause the reduction of its activity. However, they only discussed the effect of protein conformation. As in our results, the major reason for the activity reduction of RNase A is unfavorable orientation; on negatively charged surfaces, RNase A adsorbs with the "end-on" orientation, in which the catalytic active site is not accessible. Tiemeyer et al. (2010) deduced the orientation of RNase A adsorbed on COOH-SAM by the combination of reflectivity data and electron density profiles. They found that RNase A specifically coupled with

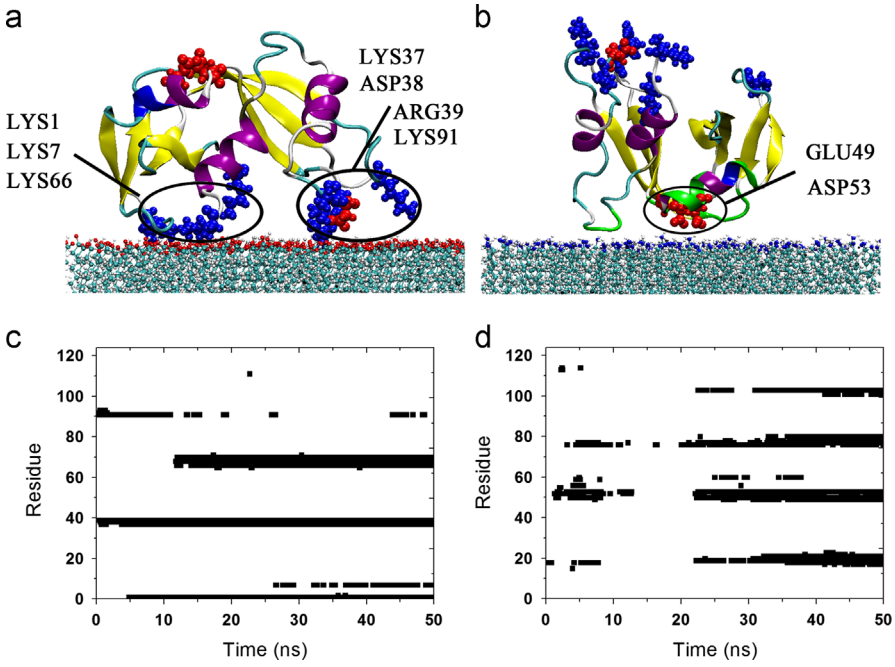

Fig. 5. The residues displaying roles in the RNase A adsorptions. Binding sites of RNase A on (a) COOH-SAM and (b) NH_2-SAM; and contact maps between RNase A and (c) COOH-SAM; (d) NH_2-SAM.

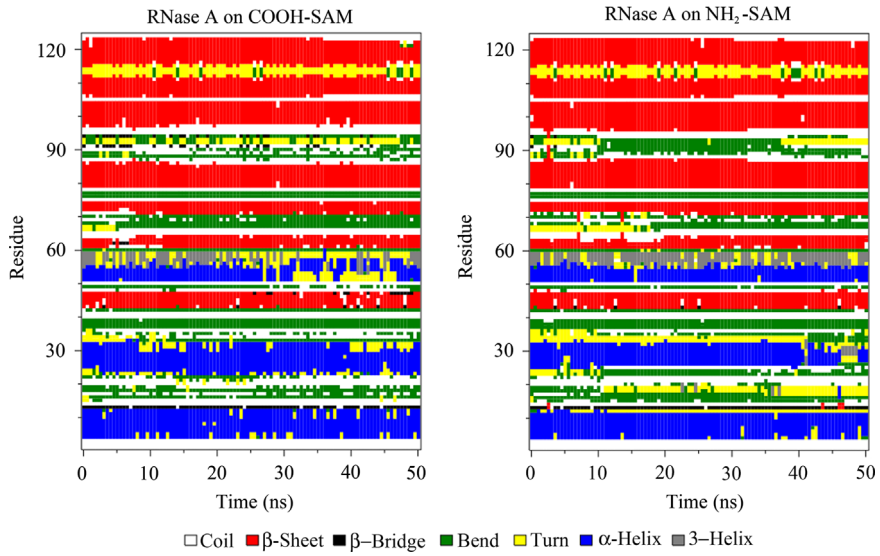

Fig. 6. Time evolution of the secondary structures of RNase A adsorbed on charged surfaces.

its active site to the negatively charged lipid monolayer, which is consistent with our result. They figured that, the orientation was supported by the fact that the main part of the positive surface charges concentrated at the active site. The electrostatic map of RNase A is shown in Fig. 4. It can be seen that the positively charged patches are distributed not only in the active site. We think that the main cause of the orientation of RNase A is not only the partial electrostatic patch, but also the direction of the dipole of RNase A. It was also mentioned in our previous works (Zhou et al., 2003, 2004b; Xie et al., 2010; Liu et al., 2013) that, the dipole of a protein was a dominant factor in determining the orientation of proteins adsorbed on charged surfaces.

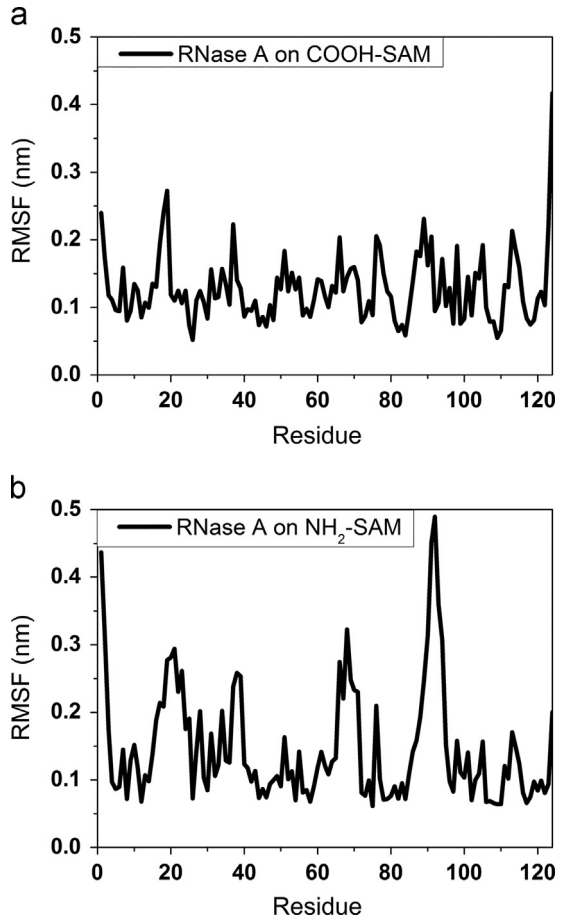

Fig. 7. The RMSF of RNase A adsorbed on COOH-SAM (a) and NH_2-SAM (b) by AAMD.

To the best of our knowledge, the orientation of RNase A on positively charged surface has not been studied by molecular simulation yet. For NH_2-SAM surface, as shown in Fig. 3, RNase A tends to adsorb with "head-on" orientation (i.e., the active site orients towards the solution). Although the net charge of RNase A is +4 e, it can adsorb on positively charged surface (as shown in Table 1 and Figs. 2 and 3). Previous researchers (Xie et al., 2010; Liu et al., 2013; Yu et al., 2014; Ravichandran et al., 2001) indicated that the net charge was not the major criterion for the protein adsorption; while the distribution of charged amino acid residues on the protein surface was the dominant factor in determining the electrostatic interactions between the protein and the surface. The dipole of the protein is the main factor to induce the protein orientation on charged surfaces. Becker et al. (2011) experimentally found that the positively charged RNase A could adsorb on a positively charged spherical polyelectrolyte brush at low ionic strengths.

Interestingly, for CG simulations at longer time scale, the orientation distribution of RNase A adsorbed on NH_2-SAM is narrower than that on COOH-SAM, as shown in Fig. 2. Although the RNase A has the same charge property as that of NH_2-SAM, it presents a more concentrated orientation. This can be explained by the local geometrical morphology of RNase A interacting with surfaces. As shown in Fig. 4, for RNase A adsorbed on the NH_2-SAM, the morphology of the protein binding patch is relatively flat than that on the COOH-SAM. As shown in Table 1, the interaction energy between RNase A and COOH-SAM is stronger than that between RNase A and NH_2-SAM. Thus, the protein orientation distribution cannot be used as the only criteria to judge whether the protein adsorption is stable. We think that the orientation distributions are determined by the dipole of the protein and the geometric feature of the protein. Also, from both AAMD and CGMD, we get consistent preferred orientations of RNase A on both surfaces, while the simulation time scale is sufficient long in CGMD simulations.

As RNase A adsorbs on different charged surfaces with opposite orientations, it can be used for different purposes. RNase A can be more strongly adsorbed on negatively charged surfaces, though without bioactivity, since the catalytic active site is blocked; however, negatively charged surfaces could be used for residual RNase A removal in solutions. To bring the enzymatic catalysis of RNase A into play, the positively charged surfaces can be used to control the orientation of RNase A with active site accessible, therefore the activity of RNase A is well utilized.

3.2. Binding sites

To investigate the process of RNase A adsorbed on surfaces, the gradual approach to the SAM surfaces and the distribution of contact

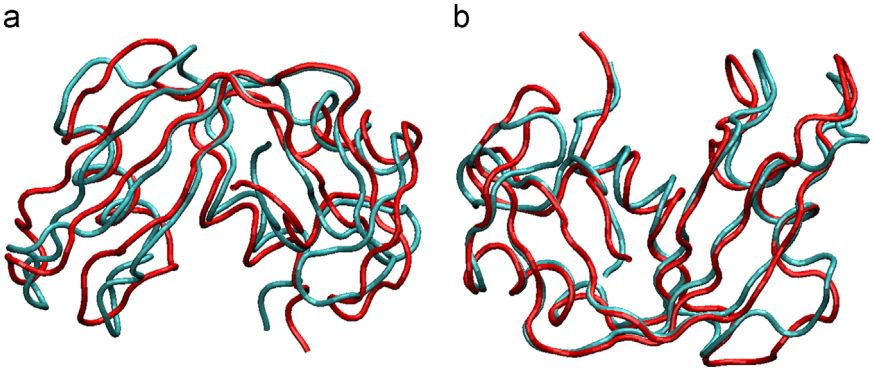

Fig. 8. Simulated structure of RNase A (in red) adsorbed on (a) COOH-SAM and (b) NH_2-SAM superimposed on the crystal structure of RNase A (in cyan). (For interpretation of the references to color in this figure legend, the reader is referred to the web version of this article.)

amino acid residues are analyzed by a map of close protein-surface contacts (Siwko and Corni, 2013); the final configurations of RNase A on charged surfaces with labeled binding sites are shown in Fig. 5. The map of the contact residues is plotted by monitoring the distance between each atom within the protein and the top layer of the surface along the *z*-direction. When such distance is less than 0.35 nm, the residue containing the corresponding atom is considered to be in contact with the surface and plotted in the map (Siwko and Corni, 2013). From the contact map of RNase A on COOH-SAM (Fig. 5c), it can be found that the protein approaching to the negatively charged surface, is induced by five positively charged residues (i.e., LYS1, LYS37, ARG39, LYS66, and LYS91) during the initial 15 ns. Then, the protein adsorbs onto the surface stably. At the end of the simulation, residues which contact with the surface are almost positively charged except for ASP38 (as is shown in Fig. 5a). It is easy to understand that the binding sites are mainly composed by positively charged residues due to the electrostatic interactions between the protein and the negatively charged surface (see Table 1). The only negatively charged residue ASP38 appearing above the surface, is mainly caused by the amino acids around it, i.e., LYS37 and ARG39. Obviously, ASP38 is pulled close to the COOH-SAM by these two positively charged residues.

As the dominant driving force of RNase A adsorbed on NH_2-SAM is quite different from that of RNase A adsorbed on COOH-SAM, the adsorption process and contact residues are also quite different. As shown in Fig. 5d, at the beginning of the AAMD simulation (i.e., during the first 20 ns), the residues cannot stably contact with the surface. From about 23 ns till to the end of the simulation, the protein is adsorbed onto the positively charged surface through SER18, ALA20, SER50, ALA52, SER77, SER80, ASN103, GLU49 and ASP53. Among these key residues, there are only two negatively charged amino acids, GLU49 and ASP53, which contribute most of the electrostatic interaction. As we have mentioned above, RNase A adsorbed on a positively charged surface is driven by vdW interactions and electrostatic interactions synergistically. It can be seen from Fig. 5b that the secondary structures near NH_2-SAM are α-helix and some random coils, which benefits from the affinity between the protein and the surface; while the secondary structures contacting to COOH-SAM are linkers between α-helix and β-sheet, which could result in a slight perturbation of the protein orientation. This result agrees well the orientation distribution that simulated by the CGMD method (as shown in Fig. 2).

3.3. Dipole moment, gyration radius and eccentricity

The dipole moment is the module of the dipole; it represents protein's charge distribution (Zhou et al., 2004a; Liu et al., 2013). The dipole moments of RNase A by different methods are averaged over the last 10 ns of the trajectories (shown in Table 2). From AAMD simulation results, the dipole moments of RNase A adsorbed on COOH-SAM and NH_2-SAM are 466 ± 12 D, 472 ± 36 D, respectively; compared with that of RNase A in bulk water, 311 ± 33 D, they are obviously larger. It is mainly caused by the charged surfaces. It is worthy of being emphasized that, the change of the dipole moment of adsorbed RNase A is mainly caused by the side chains of charged residues. Side chains of residues, with the same charge property as that of surface, tend to move away from the surface due to the repulsive electrostatic interactions. The conformation of the entire backbone of the protein is still preserved (later discussion). From Table 2, we also find that, the results from simulations at different time scales are qualitatively the same, which indicates that the properties of the protein we present here reach the adsorption equilibrium.

The same trend can also be found in gyration radius (R_{gyr}) and eccentricity (as shown in Table 2). The gyration radius of a protein represents a mass-weighted root-mean-square average distance of all atoms in a protein from its center of mass. The eccentricity is defined as $1 - I_{ave}/I_{max}$, in which I_{max} is the maximal principal moment of inertia; I_{ave} is the average of three principal moments of inertia (Zhou et al., 2004b; Liu et al., 2013). The gyration radius is usually combined with eccentricity to characterize the overall shape of a protein. Data we analyzed here are also gotten from AAMD simulations. It can be seen that, gyration radii of RNase A adsorbed on COOH-SAM (1.47 nm) and NH_2-SAM (1.48 nm) are slightly larger than that in bulk solution (1.44 nm). The eccentricities of RNase A adsorbed on charged surfaces also increase (as shown in Table 2). Bigger values of the gyration radius and the eccentricity indicate that the ellipsoidal degree of the adsorbed protein is increased, since the long axis of the adsorbed protein parallels to surfaces.

3.4. RMSD, DSSP, RMSF and superimposed structures

The conformation changes of RNase A adsorbed on charged surfaces are analyzed by root-mean-square deviation (RMSD), root-mean-square fluctuation (RMSF), definition of secondary structure of protein (DSSP) and superimposed structures. The RMSD value is calculated by comparing the backbone structure between crystal structure and the adsorbed structure. In Stocker et al.'s work (Stocker et al., 2000), they mentioned that the behavior of a protein in solution was very similar to that in its crystal environment. RMSD values of RNase A adsorbed on COOH-SAM and NH_2-SAM are 0.23 nm and 0.24 nm, respectively. They are lower when compared with that in bulk solution (0.31 nm). This means that RNase A adsorbed on surfaces experiences less structural deviations than that in bulk solution. Because the interactions between the protein and surface can cause constraints on the protein and result in the reduction of enzyme flexibility and/or alteration of the enzyme hydration shell, even without affecting the conformation significantly (Secundo, 2013). In previous works, researchers also found that the conformation deviation of protein adsorbed on surface was less than that in bulk solution (Zhao et al., 2011; Yang et al., 2014). Thus, the proteins adsorbed on charged surfaces basically maintain its native structures during the entire 50 ns AAMD simulations. It is consistent with our previous works that the conformation of proteins can be well preserved when they were adsorbed on slightly charged surfaces (Zhou et al., 2004b; Liu et al., 2013). As we have mentioned above that ellipsoidal degree of the adsorbed protein is increased, while the native conformation of backbone of RNase A is well preserved (presented by RMSD). Thus, the increase of the ellipsoidal degree is mainly caused by the side-chain of charged residues, which have opposite charges to the surface.

RMSD values from CGMD simulations are not shown here due to the Elastic Network models (Periole et al., 2009) we have used in CGMD simulations. Because of the inherent structural bias of elastic network models toward the reference configuration, the model cannot be expected to produce conformational changes skin to those necessary for a protein to fold (Periole et al., 2009). The CGMD simulations we performed here are used to study whether there is further reorientation of adsorbed protein during the microsecond time scale simulations.

As the RMSD just reveal the overall conformation change of adsorbed proteins, the local structure deviation or the change of secondary structure cannot be observed. Thus, we further analyze the DSSP (Fig. 6) and RMSF (Fig. 7) to illustrate the local conformation changes. As shown in Fig. 6, structural fluctuations mainly occur in the terminal of α-helix, coils and turns. Because these kinds of secondary structures contain less hydrogen bonds, they result in relative flexible structures that can be easily extended by external environment. The RMSF is calculated to measure the deviation between the residues and crystal structures. Fig. 7 shows the RMSF of RNase A adsorbed on COOH-SAM,

the residues near the relatively flexible structures (i.e., α-helix, coils and turn secondary structures) undergo slightly fluctuations (refer to Figs. 1 and 6), expect for VAL124 which is the C-terminus in RNase A. As the C-terminus present the same charge property as that of COOH-SAM, the deviation of C-terminus from its crystal structure is mainly induced by the electrostatic repulsion. The terminal residues can be influenced by the solvent molecules; this is also a reason for the higher RMSF of C-terminus. The same phenomenon can also be found for RNase A adsorbed on NH_2-SAM, in which the N-terminus gets a higher RMSF than other residues. For RNase A adsorbed on NH_2-SAM, except for N-terminus, LYS66 and LYS91 also experience significant changes (as shown in Fig. 7). As LYS66 and LYS91 are located in the positively charged patch in RNase A, the electrostatic repulsion could lead the positively charged residues to move away from the surface. Furthermore, LYS66 and LYS91 are also situated in the terminus of α-helix and coil secondary structures, thus it is easier for them to deviate from their initial positions.

Moreover, the final structures of RNase A adsorbed on charged surfaces are superimposed on their crystal structures (as shown in Fig. 8). It indicates that the overall conformations of proteins are basically preserved. The slight conformation changes occur in the relatively flexible secondary structures (i.e., α-helix, coils and turns). This kind of change does not affect the catalytic activity of RNase A distinctly.

4. Conclusions

We employ multiscale simulations (PTMC, CGMD and AAMD) to study the orientation and initial conformation changes of RNase A adsorbed on charged self-assembled monolayers (i.e., COOH-SAM and NH_2-SAM). The RNase A in bulk solution is also simulated as a reference system. The results are concluded as follows.

The processes of proteins adsorbed on charged surfaces are driven by the competition between electrostatic interactions and vdW interactions. The electrostatic interaction is the dominant interaction for RNase A adsorbed on COOH-SAM; while for RNase A on NH_2-SAM, the adsorption is induced by the synergy of electrostatic and vdW interactions.

RNase A can adsorb on oppositely charged SAMs with opposite orientations. The active site of RNase A is oriented toward the surface when it adsorbs on negatively charged surface; while for RNase A adsorbed on positively charged surface, the active site is oriented toward the solution. In another word, RNase A can hydrolyze RNA effectively when it adsorbs on a positively charged surface.

For RNase A adsorbed on COOH-SAM, the protein is mainly bound on the surface by positively charged residues (i.e., LYS1, LYS37, ARG39, LYS66 and LYS91); for RNase A adsorbed on NH_2-SAM, the dominant binding sites are composed of two negatively charged residues (GLU49 and ASP53) and a series of flexible secondary structures.

Although the proteins on surfaces present larger dipole moments compared with that in bulk due to the charged surfaces, the native conformations are still preserved. This has been illustrated by the analysis of RMSD, RMSF, DSSP, superimposed structures, gyration radius and eccentricity.

In general, this work sheds some lights on the mechanism of RNase A adsorption orientation and conformation on charged surfaces. We adopt model surfaces (i.e., SAMs) to illustrate the approach to control the orientation of RNase A. RNase A can be more strongly adsorbed on negatively charged surfaces, though without bioactivity, since the catalytic active site is blocked; however, negatively charged surfaces could be used for RNase A removal. To bring the enzymatic catalysis of RNase A into play, the positively charged surfaces can be used to control the orientation of RNase A with active site accessible, therefore the activity of RNase A is well utilized. These findings could contribute for the design and development of removal of RNase A from RNA solution or effective immobilization of RNase A.

Acknowledgments

This work is supported by National Key Basic Research Program of China (No. 2013CB733500), the National Natural Science Foundation of China (Nos. 21376089, 91334202), Guangdong Science Foundation (No. S2011010002078) and the Fundamental Research Funds for the Central Universities (SCUT-2013ZM0073). The computational resources for this project are provided by SCUTGrid at South China University of Technology and the ScGrid of Supercomputing Center, Computer Network Information Center of Chinese Academy of Sciences. The electrostatic profile of protein is analyzed by the UCSF Chimera package. Chimera is developed by the Resource for Biocomputing, Visualization, and Informatics at the University of California, San Francisco (supported by NIGMS P41-GM103311).

References

Agashe, M., Raut, V., Stuart, S.J., Latour, R.A., 2005. Molecular simulation to characterize the adsorption behavior of a fibrinogen gamma-chain fragment. Langmuir 21 (3), 1103–1117. http://dx.doi.org/10.1021/la0478364.

Becker, A.L., Welsch, N., Schneider, C., Ballauff, M., 2011. Adsorption of RNase A on cationic polyelectrolyte brushes: a study by isothermal titration calorimetry. Biomacromolecules 12 (11), 3936–3944. http://dx.doi.org/10.1021/bm200954j.

Camilloni, C., Robustelli, P., De Simone, A., Cavalli, A., Vendruscolo, M., 2012. Characterization of the conformational equilibrium between the two major substates of RNase A using NMR chemical Shifts. J. Am. Chem. Soc. 134 (9), 3968–3971. http://dx.doi.org/10.1021/ja210951z.

Chatterjee, S., Debenedetti, P.G., Stillinger, F.H., Lynden-Bell, R.M., 2008. A computational investigation of thermodynamics, structure, dynamics and solvation behavior in modified water models. J. Chem. Phys. 128 (12), 124511. http://dx.doi.org/10.1063/1.2841127.

Cooke, G.D., Cranenburgh, R.M., Hanak, J.A.J., Dunnill, P., Thatcher, D.R., Ward, J.M., 2001. Purification of essentially RNA free plasmid DNA using a modified *Escherichia coli* host strain expressing ribonuclease A. J. Biotechnol. 85 (3), 297–304. http://dx.doi.org/10.1016/s0168-1656(00)00378-3.

Cuchillo, C.M., Victoria Nogues, M., Raines, R.T., 2011. Bovine pancreatic ribonuclease: fifty years of the first enzymatic reaction mechanism. Biochemistry. 50 (37), 7835–7841. http://dx.doi.org/10.1021/bi201075b.

Cullen, S.P., Liu, X., Mandel, I.C., Himpsel, F.J., Gopalan, P., 2008. Polymeric brushes as functional templates for immobilizing ribonuclease A: Study of binding kinetics and activity. Langmuir 24 (3), 913–920. http://dx.doi.org/10.1021/la702510z.

Eon-Duval, A., Burke, G., 2004. Purification of pharmaceutical-grade plasmid DNA by anion-exchange chromatography in an RNase-free process. J. Chromatogr. B 804 (2), 327–335. http://dx.doi.org/10.1016/j.jchromb.2004.01.033.

Essmann, U., Perera, L., Berkowitz, M.L., Darden, T., Hsing, L., Pedersen, L.G., 1995. A smooth particle mesh Ewald method. J. Chem. Phys. 103 (19), 8577–8593. http://dx.doi.org/10.1063/1.470117.

Findlay, D., Herries, D.G., Mathias, A.P., Rabin, B.R., Ross, C.A., 1961. The active site and mechanism of action of bovine pancreatic ribonuclease. Nature 190, 781–784. http://dx.doi.org/10.1038/190781a0.

Glennon, T.M., Warshel, A., 1998. Energetics of the catalytic reaction of ribonuclease A: A computational study of alternative mechanisms. J. Am. Chem. Soc. 120 (39), 10234–10247. http://dx.doi.org/10.1021/ja981594x.

Hess, B., Bekker, H., Berendsen, H.J.C., Fraaije, J., 1997. LINCS: a linear constraint solver for molecular simulations. J. Comput. Chem. 18 (12), 1463–1472. http://dx.doi.org/10.1002/(sici)1096-987x(199709)18:12<1463::aid-jcc4>3.3.co;2-h.

Hess, B., Kutzner, C., van der Spoel, D., Lindahl, E., 2008. GROMACS 4: algorithms for highly efficient, load-balanced, and scalable molecular simulation. J. Chem. Theory Comput. 4 (3), 435–447. http://dx.doi.org/10.1021/ct700301q.

Hoover, W.G., 1985. Canonical dynamics: equilibrium phase-space distributions. Phys. Rev. A 31 (3), 1695–1697.

Hsu, H.J., Sheu, S.Y., Tsay, R.Y., 2008. Preferred orientation of albumin adsorption on a hydrophilic surface from molecular simulation. Colloid Surf. B 67 (2), 183–191. http://dx.doi.org/10.1016/j.colsurfb.2008.08.017.

Humphrey, W., Dalke, A., Schulten, K., 1996. VMD: visual molecular dynamics. J. Mol. Graphics 14 (1), 33–38. http://dx.doi.org/10.1016/0263-7855(96)00018-5.

Hung, A., Mwenifumbo, S., Mager, M., Kuna, J.J., Stellacci, F., Yarovsky, I., Stevens, M.M., 2011. Ordering surfaces on the nanoscale: Implications for protein adsorption. J. Am. Chem. Soc. 133 (5), 1438–1450. http://dx.doi.org/10.1021/ja108285u.

Ji, C.G., Zhang, J.Z.H., 2011. Understanding the molecular mechanism of enzyme dynamics of ribonuclease A through protonation/deprotonation of HIS48. J. Am. Chem. Soc. 133 (44), 17727–17737. http://dx.doi.org/10.1021/ja206212a.
Kaminski, G.A., Friesner, R.A., Tirado-Rives, J., Jorgensen, W.L., 2001. Evaluation and reparametrization of the OPLS-AA force field for proteins via comparison with accurate quantum chemical calculations on peptides. J. Phys. Chem. B 105 (28), 6474–6487. http://dx.doi.org/10.1021/jp003919d.
Khan, M.S., Garnier, G., 2013. Direct measurement of alkaline phosphatase kinetics on bioactive paper. Chem. Eng. Sci. 87, 91–99. http://dx.doi.org/10.1016/j.ces.2012.09.022.
Kony, D., Damm, W., Stoll, S., van Gunsteren, W.F., 2002. An improved OPLS-AA force field for carbohydrates. J. Comput. Chem. 23 (15), 1416–1429. http://dx.doi.org/10.1002/jcc.10139.
Lee, C.S., Belfort, G., 1989. Changing activity of ribonuclease A during adsorption: a molecular explanation. Proc. Nat. Acad. Sci. USA 86 (21), 8392–8396. http://dx.doi.org/10.1073/pnas.86.21.8392.
Liang, J., Fieg, G., Keil, F.J., Jakobtorweihen, S., 2012. Adsorption of proteins onto ion-exchange chromatographic media: a molecular dynamics study. Ind. Eng. Chem. Res. 51 (49), 16049–16058. http://dx.doi.org/10.1021/ie301407b.
Liu, J., Liao, C., Zhou, J., 2013. Multiscale simulations of protein G B1 adsorbed on charged self-assembled monolayers. Langmuir 29 (36), 11366–11374. http://dx.doi.org/10.1021/la401171v.
Lopez, C.A., Rzepiela, A.J., de Vries, A.H., Dijkhuizen, L., Hunenberger, P.H., Marrink, S.J., 2009. Martini coarse-grained force field: Extension to carbohydrates. J. Chem. Theory Comput. 5 (12), 3195–3210. http://dx.doi.org/10.1021/ct900313w.
Lopez, C.A., Sovova, Z., van Eerden, F.J., De Vries, A.H., Marrink, S.J., 2013. Martini force field parameters for glycolipids. J. Chem. Theory Comput. , http://dx.doi.org/10.1021/ct3009655.
Marrink, S.J., de Vries, A.H., Mark, A.E., 2003. Coarse grained model for semiquantitative lipid simulations. J. Phys. Chem. B 108 (2), 750–760. http://dx.doi.org/10.1021/jp036508g.
Marrink, S.J., Risselada, H.J., Yefimov, S., Tieleman, D.P., de Vries, A.H., 2007. The MARTINI force field: coarse grained model for biomolecular simulations. J. Phys. Chem. B 111 (27), 7812–7824. http://dx.doi.org/10.1021/jp071097f.
Merlino, A., Vitagliano, L., Ceruso, M.A., Di Nola, A., Mazzarella, L., 2002. Global and local motions in ribonuclease A: A molecular dynamics study. Biopolymers 65 (4), 274–283. http://dx.doi.org/10.1002/bip.10225.
Mijajlovic, M., Biggs, M.J., 2007. On use of the amber potential with the Langevin dipole method. J. Phys. Chem. B 111 (26), 7591–7602. http://dx.doi.org/10.1021/jp0701744.
Mijajlovic, M., Penna, M.J., Biggs, M.J., 2013. Free energy of adsorption for a peptide at a liquid/solid interface via nonequilibrium molecular dynamics. Langmuir 29 (9), 2919–2926. http://dx.doi.org/10.1021/la3047966.
Monticelli, L., Kandasamy, S.K., Periole, X., Larson, R.G., Tieleman, D.P., Marrink, S.J., 2008. The MARTINI coarse-grained force field: extension to proteins. J. Chem. Theory Comput. 4 (5), 819–834. http://dx.doi.org/10.1021/ct700324x.
Nordgren, C.E., Tobias, D.J., Klein, M.L., Blasie, J.K., 2002. Molecular dynamics simulations of a hydrated protein vectorially oriented on polar and nonpolar soft surfaces. Biophys. J. 83 (6), 2906–2917.
Nose, S., 1984. A unified formulation of the constant temperature molecular dynamics methods. J. Chem. Phys. 81 (1), 511–519.
Ostuni, E., Yan, L., Whitesides, G.M., 1999. The interaction of proteins and cells with self-assembled monolayers of alkanethiolates on gold and silver. Colloid Surf. B 15 (1), 3–30. http://dx.doi.org/10.1016/s0927-7765(99)00004-1.
Periole, X., Cavalli, M., Marrink, S.-J., Ceruso, M.A., 2009. Combining an elastic network with a coarse-grained molecular force field: Structure, dynamics, and intermolecular recognition. J. Chem. Theory Comput. 5 (9), 2531–2543. http://dx.doi.org/10.1021/ct9002114.
Pettersen, E.F., Goddard, T.D., Huang, C.C., Couch, G.S., Greenblatt, D.M., Meng, E.C., Ferrin, T.E., 2004. UCSF chimera – a visualization system for exploratory research and analysis. J. Comput. Chem. 25 (13), 1605–1612. http://dx.doi.org/10.1002/jcc.20084.
Ravichandran, S., Madura, J.D., Talbot, J., 2001. A Brownian dynamics study of the initial stages of hen egg-white lysozyme adsorption at a solid interface. J. Phys. Chem. B 105 (17), 3610–3613. http://dx.doi.org/10.1021/jp010223r.
Secundo, F., 2013. Conformational changes of enzymes upon immobilisation. Chem. Soc. Rev. 42 (15), 6250–6261. http://dx.doi.org/10.1039/c3cs35495d.
Shang, W., Nuffer, J.H., Dordick, J.S., Siegel, R.W., 2007. Unfolding of ribonuclease A on silica nanoparticle surfaces. Nano Lett. 7 (7), 1991–1995. http://dx.doi.org/10.1021/nl070777r.
Sheng, Y.B., Wang, W., Chen, P., 2010. Adsorption of an ionic complementary peptide on the hydrophobic graphite surface. J. Phys. Chem. C 114 (1), 454–459. http://dx.doi.org/10.1021/jp908629g.
Shrivastava, S., Nuffer, J.H., Siegel, R.W., Dordick, J.S., 2012. Position-specific chemical modification and quantitative proteomics disclose protein orientation adsorbed on silica nanoparticles. Nano Lett. 12 (3), 1583–1587. http://dx.doi.org/10.1021/nl2044524.
Siwko, M.E., Corni, S., 2013. Cytochrome C on a gold surface: Investigating structural relaxations and their role in protein-surface electron transfer by molecular dynamics simulations. Phys. Chem. Chem. Phys. 15 (16), 5945–5956. http://dx.doi.org/10.1039/c3cp00146f.
Smith, B.D., Soellner, M.B., Raines, R.T., 2005. Synthetic surfaces for ribonuclease adsorption. Langmuir 21 (1), 187–190. http://dx.doi.org/10.1021/la0480686.
Stocker, U., Spiegel, K., van Gunsteren, W.F., 2000. On the similarity of properties in solution or in the crystalline state: a molecular dynamics study of hen lysozyme. J. Biomol. NMR 18 (1), 1–12. http://dx.doi.org/10.1023/a:1008379605403.
Tiemeyer, S., Paulus, M., Tolan, M., 2010. Effect of surface charge distribution on the adsorption orientation of proteins to lipid monolayers. Langmuir 26 (17), 14064–14067. http://dx.doi.org/10.1021/la102616h.
Trzaskowski, B., Leonarski, F., Les, A., Adamowicz, L., 2005. Modeling tubulin at interfaces. immobilization of microtubules on self-assembled monolayers. J. Phys. Chem. B 109 (37), 17734–17742. http://dx.doi.org/10.1021/jp052015v.
Trzaskowski, B., Leonarski, F., Les, A., Adamowicz, L., 2008. Altering the orientation of proteins on self-assembled monolayers: a computational study. Biomacromolecules 9 (11), 3239–3245. http://dx.doi.org/10.1021/bm800806n.
Wang, H., He, Y., Ratner, B.D., Jiang, S.Y., 2006. Modulating cell adhesion and spreading by control of FnIII(7–10) orientation on charged self-assembled monolayers (SAMs) of alkanethiolates. J. Biomed. Mater. Res. Part A 77A (4), 672–678. http://dx.doi.org/10.1002/jbm.a.30586.
Wei, T., Carignano, M.A., Szleifer, I., 2011. Lysozyme adsorption on polyethylene surfaces: why are long simulations needed? Langmuir 27 (19), 12074–12081. http://dx.doi.org/10.1021/la202622s.
Wittemann, A., Ballauff, M., 2005. Temperature-induced unfolding of ribonuclease – a embedded in spherical polyelectrolyte brushes. Macromol. Biosci. 5 (1), 13–20. http://dx.doi.org/10.1002/mabi.200400133.
Wlodawer, A., Svensson, L.A., Sjolin, L., Gilliland, G.L., 1988. Structure of phosphate-free ribonuclease A refined at 1.26 A. Biochemistry 27 (8), 2705–2717. http://dx.doi.org/10.1021/bi00408a010.
Wu, Z., Cui, Q.A., Yethiraj, A., 2010. A New coarse-grained model for water: the importance of electrostatic interactions. J. Phys. Chem. B 114 (32), 10524–10529. http://dx.doi.org/10.1021/jp1019763.
Wu, Z., Cui, Q., Yethiraj, A., 2011. A new coarse-grained force field for membrane-peptide simulations. J. Chem. Theory Comput. 7 (11), 3793–3802. http://dx.doi.org/10.1021/ct200593t.
Xie, Y., Zhou, J., Jiang, S.Y., 2010. Parallel tempering Monte Carlo simulations of lysozyme orientation on charged surfaces. J. Chem. Phys. 132 (6), 065101. http://dx.doi.org/10.1063/1.3305244.
Xie, Y., Liu, M.F., Zhou, J., 2012. Molecular dynamics simulations of peptide adsorption on self-assembled monolayers. Appl. Surf. Sci. 258 (20), 8153–8159. http://dx.doi.org/10.1016/j.apsusc.2012.05.013.
Xie, Y., Liao, C., Zhou, J., 2013. Effects of external electric fields on lysozyme adsorption by molecular dynamics simulations. Biophys. Chem. 179 (0), 26–34. http://dx.doi.org/10.1016/j.bpc.2013.05.002.
Yang, C., Peng, C., Zhao, D., Liao, C., Zhou, J., Lu, X., 2014. Molecular simulations of myoglobin adsorbed on rutile (110) and (001) surfaces. Fluid Phase Equilib. 362, 349–354. http://dx.doi.org/10.1016/j.fluid.2013.10.052.
Yeh, I.C., Berkowitz, M.L., 1999. Ewald summation for systems with slab geometry. J. Chem. Phys. 111 (7), 3155–3162. http://dx.doi.org/10.1063/1.479595.
Yi, C., Fong, C.-C., Zhang, Q., Lee, S.-T., Yang, M., 2008. The structure and function of ribonuclease A upon interacting with carbon nanotubes. Nanotechnology 19 (9), 095102. http://dx.doi.org/10.1088/0957–4484/19/9/095102.
Yu, G.B., Liu, J., Zhou, J., 2014. Mesoscopic coarse-grained simulations of lysozyme adsorption. J. Phys. Chem. B , http://dx.doi.org/10.1021/jp409326f.
Yu, X., Wang, Q.M., Lin, Y.A., Zhao, J., Zhao, C., Zheng, J., 2012. Structure, orientation, and surface interaction of alzheimer amyloid-beta peptides on the graphite. Langmuir 28 (16), 6595–6605. http://dx.doi.org/10.1021/la3002306.
Zhang, A.J., Xie, Y., Zhou, J., 2009. Experimental control and characterization of protein orientation on surfaces. Prog. Chem. 21 (7–8), 1408–1417.
Zhao, J., Wang, Q., Liang, G., Zheng, J., 2011. Molecular dynamics simulations of low-ordered alzheimer beta-amyloid oligomers from dimer to hexamer on self-assembled monolayers. Langmuir *27* (24), 14876–14887. http://dx.doi.org/10.1021/la2027913.
Zhou, J., Chen, S.F., Jiang, S.Y., 2003. Orientation of adsorbed antibodies on charged surfaces by computer simulation based on a united-residue model. Langmuir *19* (8), 3472–3478. http://dx.doi.org/10.1021/la026871z.
Zhou, J., Zheng, J., Jiang, S.Y., 2004b. Molecular simulation studies of the orientation and conformation of cytochrome c adsorbed on self-assembled monolayers. J. Phys. Chem. B 108 (45), 17418–17424. http://dx.doi.org/10.1021/jp038048x.
Zhou, J., Tsao, H.K., Sheng, Y.J., Jiang, S.Y., 2004a. Monte Carlo simulations of antibody adsorption and orientation on charged surfaces. J. Chem. Phys. 121 (2), 1050–1057. http://dx.doi.org/10.1063/1.1757434.